

Communication

Tunable Luminescence of $\text{Sm}^{3+}/\text{Tb}^{3+}$ Co-Doped CaMoO_4 Phosphors Synthesized by Microwave-Assisted Heating

Wen-Te Wu ¹, Kwong-Kau Tiong ¹, Yu-Wei Lee ¹, Sheng-Yao Hu ², Yueh-Chien Lee ^{3,*}  and Wei Huang ³¹ Department of Electrical Engineering, National Taiwan Ocean University, Keelung 202, Taiwan² Department of Electrical Engineering, Lunghwa University of Science and Technology, Guishan, Taoyuan 333, Taiwan³ Department of Electronic Engineering, Tunghua University, Shenkeng, New Taipei 222, Taiwan

* Correspondence: jacklee@mail.tnu.edu.tw

Abstract: We present a series of $\text{Sm}^{3+}/\text{Tb}^{3+}$ co-doped CaMoO_4 phosphors synthesized by an efficient method of microwave-assisted heating. The prepared CaMoO_4 samples were characterized by X-ray diffraction, photoluminescence, and Commission Internationale de l'Éclairage (CIE) chromaticity diagram. The X-ray diffraction results confirmed that all synthesized CaMoO_4 samples are crystallized in a pure tetragonal phase. The photoluminescence spectra significantly show both red- and green emissions in the synthesized $\text{Sm}^{3+}/\text{Tb}^{3+}$ co-doped CaMoO_4 phosphors. It is obvious that the variations in the intensity ratio of red/green emissions depend on the molar ratio of $\text{Sm}^{3+}/\text{Tb}^{3+}$ co-doping and dominate the CIE color coordinates on the chromaticity diagram. The investigations showed the functionality of the material system as advanced color-tunable phosphors for white-LEDs as evidenced by the controllability of the light-emitting region of $\text{Sm}^{3+}/\text{Tb}^{3+}$ co-doped CaMoO_4 phosphors through the adjustment of the molar ratio of $\text{Sm}^{3+}/\text{Tb}^{3+}$ ions.



Citation: Wu, W.-T.; Tiong, K.-K.; Lee, Y.-W.; Hu, S.-Y.; Lee, Y.-C.; Huang, W. Tunable Luminescence of $\text{Sm}^{3+}/\text{Tb}^{3+}$ Co-Doped CaMoO_4 Phosphors Synthesized by Microwave-Assisted Heating. *Appl. Sci.* **2022**, *12*, 7883. <https://doi.org/10.3390/app12157883>

Keywords: CaMoO_4 ; microwave-assisted synthesis; X-ray diffraction; photoluminescence

PACS: 61.46.-w; 78.55.-m; 81.20.-n

Academic Editors: Antonio Di Bartolomeo and Marilou Cadatal Raduban

Received: 10 June 2022

Accepted: 3 August 2022

Published: 5 August 2022

Publisher's Note: MDPI stays neutral with regard to jurisdictional claims in published maps and institutional affiliations.



Copyright: © 2022 by the authors. Licensee MDPI, Basel, Switzerland. This article is an open access article distributed under the terms and conditions of the Creative Commons Attribution (CC BY) license (<https://creativecommons.org/licenses/by/4.0/>).

1. Introduction

Recently, molybdate compounds given by the general formula XMoO_4 with $\text{X} = \text{Ca}, \text{Ba}, \text{Pb}, \text{Li}, \text{Zn},$ or Sr have shown great applications as host material for solid state optical lasers, optical fibers, magnetic materials, light-emitting diodes (LEDs), etc. [1–5]. Among metal molybdate compounds, calcium molybdate (CaMoO_4) material belonging to the tetragonal structure with the space group $I4_1/a$ has attracted significant attention as an excellent phosphor host because of its attractive structural properties, showing good chemical and heat stabilities which can be developed as highly applicable luminescent materials [6,7]. In the CaMoO_4 lattices, the $[\text{MoO}_4]$ polyhedral is formed by four oxygen ions coordinated to a Mo ion, whereas the $[\text{CaO}_8]$ polyhedral is formed through the coordination of eight oxygen ions to one Ca ion. It is generally known that the $(\text{MoO}_4)^{2-}$ complex allows the charge transfer (CT) from oxygen to the metal, which would facilitate the intense absorption bands in the near-ultraviolet (UV) region to emit a broad blue-green luminescence emission peak in the wavelength range of 350–650 nm at room temperature [8,9].

By further incorporating a small concentration of rare-earth ions ($\text{RE}^{3+} = \text{Tb}^{3+}, \text{Sm}^{3+},$ and Eu^{3+}) into the CaMoO_4 phosphors, the trivalent rare-earth ions can substitute for the Ca cation, resulting in a structural distortion of the $[\text{MoO}_4]$ and $[\text{CaO}_8]$ cluster chains. The structural distortion gave rise to the intermediate defect energy levels in the band gap, which can favor prominent PL emissions.

The RE^{3+} -doped CaMoO_4 phosphors absorb the UV range photons and then transfer the photon energy to the higher energy levels of RE^{3+} , and the intra configurational $f \rightarrow f$ transitions of RE^{3+} can give rise to a significant dopant dependent green (Tb^{3+}), orange-red

(Sm³⁺) and red (Eu³⁺) emission [8,9]. Based on energy transfer mechanism, co-doped phosphors have been extensively studied because of their enhanced luminescent properties. It can be expected that the RE³⁺ (Sm³⁺/Tb³⁺) co-doped CaMoO₄ phosphors should have the advantage of tunable multicolor emissions, which can be exploited and developed as an advanced phosphor applied in white-LEDs [10,11].

Several methods, such as a microwave-assisted heating method [9], precipitation [10,11], hydrothermal process [12,13], ionic liquid-assisted process [14], and sol-gel [15] have been developed to synthesize the CaMoO₄ phosphors. Among the different techniques, the microwave-assisted synthesis is the most viable method because it is a relatively fast and easy to operate process. The inherent character of the method also makes it fairly energy efficient, leading to low fabrication costs so that high yield for large scale industrial production may be realized. Moreover, the polar solvent-free system is eco-friendly so that environmental pollution may be avoided. In addition, compared to the numerous research focusing on Tb³⁺ ion as a sensitizer for enhancing the emission intensity of Eu³⁺ ion [16,17], there are only few results on the co-doping of the Tb³⁺ ion and Sm³⁺ ion. Based on the few available experimental results, the ability to tune the intensity ratio of the red/green emissions of the Sm³⁺/Tb³⁺ co-doped CaMoO₄ had been demonstrated. Nevertheless, more exploratory experimental works are warranted in this area so that a better controllability of the tuning process may be attained and a better understanding of the process can be realized. Therefore, in this paper, we present the Sm³⁺-doped, Tb³⁺-doped, and Sm³⁺/Tb³⁺ co-doped CaMoO₄ phosphors prepared by microwave-assisted heating method. The structural characteristic, luminescence property, and optical performance of the synthesized CaMoO₄ phosphors were investigated by X-ray diffraction (XRD), photoluminescence (PL), and Commission Internationale de l'Éclairage (CIE) chromaticity diagram, respectively. The variations in the measured data with the controlled molar ratio of Sm³⁺/Tb³⁺ co-doped CaMoO₄ phosphors were analyzed and discussed.

2. Materials and Methods

In this work, the Na₂MoO₄ and Ca(NO₃)₂ were used as the precursors for synthesizing Ca-MoO₄ phosphors via microwave-assisted heating [9,18]. The weighted Na₂MoO₄ and Ca(NO₃)₂ were separately dissolved in distilled water, and then mixed together. The mixture was vigorously stirred at room temperature for 30 min to obtain a well-dissolved solution. The solution was then heated to 95 °C for 60 min in a microwave oven with a controlled power of 500 W. After the heating process, the mixture was slowly cooled to room temperature. The cooled solution was then placed in a centrifuge to extract the CaMoO₄ phosphors. The extracted CaMoO₄ phosphors were washed with distilled water to purify and finally dried in a furnace at 60 °C for 4 h. The aforementioned process was repeated for preparation of a series of Sm³⁺/Tb³⁺ co-doped CaMoO₄ phosphors by carefully controlling the molar ratio of Sm³⁺ and Tb³⁺ ions.

The crystalline characterization of the prepared CaMoO₄ phosphors was carried out by the XRD (Shimadzu XRD-6000) with a CuKα line of 1.5405 Å. The PL measurements were conducted using the 377 nm excitation. The luminescence was collected using a spectrometer (Zolix omni-500) with a 1200 grooves/mm grating and detected using a photomultiplier (PMT). The PL signals obtained from the PMT were analyzed using lock-in technique and recorded on a computer. Janis Research Model CCS-150 and LakeShore Model 321 temperature controller were used to measure the 12 and 300 K PL spectra. The CIE coordinates were calculated by using the PL data based on the CIE 1931 standard colorimetric system.

3. Results

Figure 1a presents the XRD pattern of the undoped-CaMoO₄ and CaMoO₄ co-doped with different molar ratios of Sm³⁺/Tb³⁺. Compared to the crystallographic JCPDS card No. 290351 [9,18], the significant diffraction peaks at 2θ = 18.6°, 28.7°, 31.2°, 34.3°, 47.0°, and 58.0° correspond to the (101), (112), (004), (200), (204), and (312) peak of CaMoO₄,

respectively. For the undoped- CaMoO_4 , no impurity peak of other phases is observed, indicating that the undoped- CaMoO_4 samples crystallized in a rather pristine tetragonal structure [9,18]. Additionally, it is noted that for the present measured XRD, after the doping of Sm^{3+} , Tb^{3+} , and the co-doping of $\text{Sm}^{3+}/\text{Tb}^{3+}$ ions, no significant variations in all the major diffraction peaks were observed. Nevertheless, a careful analysis of the most significant peak of (112), as shown in Figure 1b, has indicated that the introduction of RE^{3+} cation has induced a downshift of the (112) peak to lower angle. This observation is in line with that of Ref. [17], *viz.*, increasing shift with increasing concentration. Tranquilin et al. claimed that the variations in the (112) peak are due to the structural distortions leading to polarization in the $[\text{CaO}_8]$ clusters, which are induced from the difference between electronic densities of the Ca^{2+} in relation to the incorporated RE^{3+} cation. The schematic structure diagram of the $\text{Sm}^{3+}/\text{Tb}^{3+}$ co-doped CaMoO_4 is also depicted in the Figure 1b [17]. The results indicate that CaMoO_4 phosphors with different molar ratios of $\text{Sm}^{3+}/\text{Tb}^{3+}$ -co-doping have successfully synthesized by microwave-assisted heating [18].

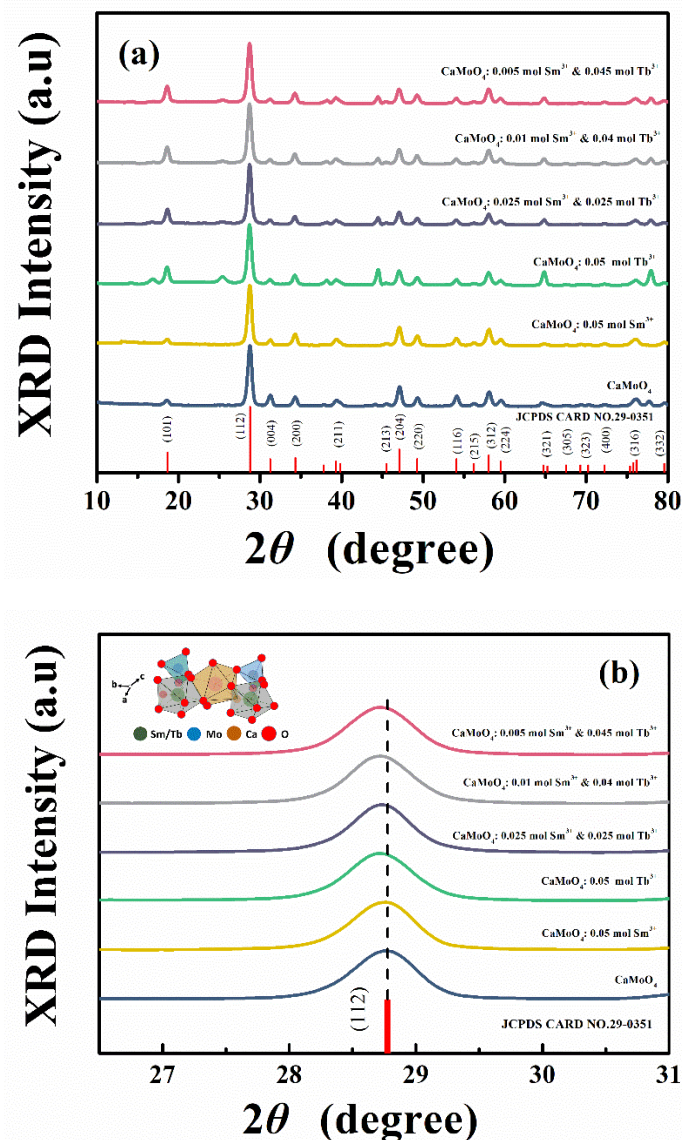


Figure 1. (a) The XRD patterns and (b) enlarged view of (112) peak of undoped- CaMoO_4 and $\text{Sm}^{3+}/\text{Tb}^{3+}$ co-doped CaMoO_4 with different molar ratios of $\text{Sm}^{3+}/\text{Tb}^{3+}$ ions.

The 12 and 300 K PL spectra of the undoped- CaMoO_4 phosphors measured under 377 nm excitation are shown in Figure 2. Both spectra show a broad-band emission

covering the visible electromagnetic spectrum in the wavelength region ranging from 425 to 600 nm. It is known that the profile of broad-band emission is due to multi-level and multi-phonon processes, where several paths involving the participation of multiple energy states exist within the band gap. For CaMoO_4 materials, the charge–transfer transitions in the intermediate levels of the band gap resulting in the broad PL spectra have been attributed to the structural and electronic distortion in the tetrahedral $(\text{MoO}_4)^{2-}$ complex ions [6,7].

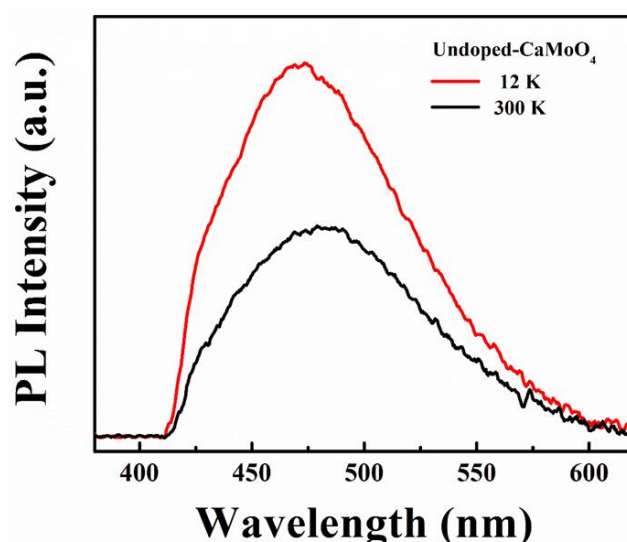


Figure 2. 12 and 300 K PL spectra of undoped- CaMoO_4 phosphors.

Figure 3a,b shows the 12 and 300 K PL spectra of 0.05 mol Sm^{3+} - and 0.05 mol Tb^{3+} -doped CaMoO_4 phosphors, respectively. The luminescence mechanisms of the RE^{3+} -doped samples are presented to provide some insight to the observed emission lines. Under UV excitation, the excited electrons in $(\text{MoO}_4)^{2-}$ group would transfer directly from the $(\text{MoO}_4)^{2-}$ complex to the high-level excited states of Sm^{3+} and Tb^{3+} via the energy transfer process. The electrons absorb energy and are promoted from the ground state $^6\text{H}_{5/2}$ of Sm^{3+} ($^7\text{F}_6$ of Tb^{3+}) to the higher level excited states, and subsequently relax to the lower $^4\text{G}_{5/2}$ of Sm^{3+} ($^5\text{D}_4$ of Tb^{3+}) level via a non-radiative process. Finally, the electrons in the populated level would undergo transition by radiative process from $^4\text{G}_{5/2}$ to $^6\text{H}_j$ ($j = 5/2, 7/2, 9/2$) for Sm^{3+} and from $^5\text{D}_4$ to $^7\text{F}_j$ ($j = 6, 5, 4, 3$) for Tb^{3+} .

Figure 3a shows the 12 K PL of 0.05 mol Sm^{3+} -doped CaMoO_4 phosphors, the significant peaks at about 563, 607, and 646 nm are attributed to the $^4\text{G}_{5/2} \rightarrow ^6\text{H}_{5/2}$, $^4\text{G}_{5/2} \rightarrow ^6\text{H}_{7/2}$, and $^4\text{G}_{5/2} \rightarrow ^6\text{H}_{9/2}$ transitions, respectively [9,18,19]. It is known that the two transitions ($^4\text{G}_{5/2} \rightarrow ^6\text{H}_{5/2, 7/2}$) contain both electric and magnetic dipole transitions, and the $^4\text{G}_{5/2} \rightarrow ^6\text{H}_{9/2}$ transition belongs to the electronic dipole transition. Moreover, the most intense emission peak at 646 nm in the red region is sensitive to the variation of the local structure environment of the Sm^{3+} ions.

On the other hands, the marked PL peaks of 0.05 mol Tb^{3+} -doped CaMoO_4 phosphors at 489, 544, 588, and 621 nm shown in Figure 3b correspond to the transitions from $^5\text{D}_4 \rightarrow ^7\text{F}_6$, $^5\text{D}_4 \rightarrow ^7\text{F}_5$, $^5\text{D}_4 \rightarrow ^7\text{F}_4$, and $^5\text{D}_4 \rightarrow ^7\text{F}_3$ of Tb^{3+} ions, respectively [18]. Two significant peaks from the $^5\text{D}_4 \rightarrow ^7\text{F}_6$ transition (blue emission) and $^5\text{D}_4 \rightarrow ^7\text{F}_5$ transition (green emission) are related to the electric dipole transition and magnetic dipole transition, respectively [20,21]. Kaur et al. further indicate that the $^5\text{D}_4 \rightarrow ^7\text{F}_6$ transition depends on the local environment and on the symmetry of crystal field, whereas the $^5\text{D}_4 \rightarrow ^7\text{F}_5$ transition is independent of the crystal field strength [21]. Moreover, the current PL measurements of the RE^{3+} -doped CaMoO_4 phosphors showed a complete quenching of the broad band emission from $(\text{MoO}_4)^{2-}$ complex ions, as observed in undoped- CaMoO_4

phosphors, indicating that the absorbed energy of the host has efficiently transferred to the activators [22].

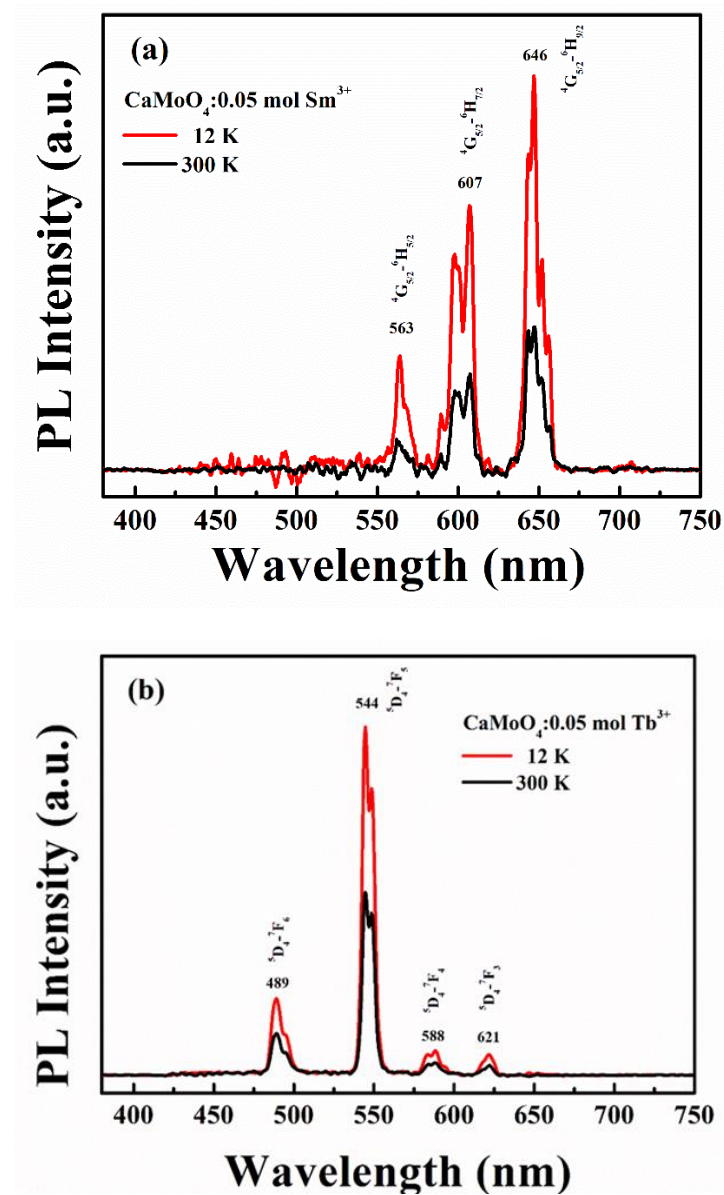


Figure 3. PL spectra of CaMoO_4 phosphors doped (a) 0.05 mol Sm^{3+} ions and (b) 0.05 mol Tb^{3+} ions.

The controllability of the PL emission lines in the visible range on the dopant concentrations have been carried out. The 12 and 300 K PL experimental measurements of $\text{Sm}^{3+}/\text{Tb}^{3+}$ co-doped CaMoO_4 phosphors with controlled molar ratio of (a) 0.05:0, (b) 0.025:0.025, (c) 0.01:0.04, (d) 0.005/0.045, and (e) 0:0.05 were performed and the spectra plotted in Figure 4.

The identification of the spectral features, as observed in Figure 4, can be performed by a careful comparison with the observed features in Figure 3. As have been described earlier, the PL peaks at 563, 607, and 646 nm are due to the transitions of Sm^{3+} ions (marked as ★), and the PL peaks at 489 and 544 nm are due to the transitions of Tb^{3+} ions (marked as ※). Clearly, the measured data of the co-doped sample as depicted by Figure 4 displayed features that can be correlated to the transitions of either Sm^{3+} ions or Tb^{3+} ions. Specifically, the PL spectra of (b)~(d) in Figure 4, which belong to the synthesized $\text{Sm}^{3+}/\text{Tb}^{3+}$ co-doped CaMoO_4 phosphors, have demonstrated the ability of the mixed samples to emit both red- and green-luminescence. Our PL measurement results for the

$\text{Sm}^{3+}/\text{Tb}^{3+}$ co-doped CaMoO_4 phosphors also showed tunability of the intensity of the visible emission peaks through varying the molar ratio of the doped $\text{Sm}^{3+}/\text{Tb}^{3+}$ ions. As indicated by the PL spectra of Figure 4, a decrease in the concentration of Sm^{3+} ions to 0.01 mol, while increasing that of Tb^{3+} ions to 0.04 mol, led to a significant enhancement of the emission intensity of 489 and 544 nm lines originated from Tb^{3+} ions, over that of the Sm^{3+} -related features. Likewise, the Sm^{3+} -related features can also be made prominent by increasing its concentration. Spectra (d) in Figure 4 showed that by decreasing the concentration of Sm^{3+} ions to 0.005 mol and increasing that of Tb^{3+} ions to 0.045 mol, the emission intensity of Tb^{3+} -related features at 489 and 544 nm dominate over that of Sm^{3+} -related features at 563, 607, and 646 nm. The ability to tune the peak intensity of 646 nm (red-emission) and 544 nm (green-emission), *viz.*, the controllability of the color emission of CaMoO_4 phosphors through the adjustment of the molar ratio of the two rare-earth ions of Sm^{3+} and Tb^{3+} [23,24] show immense potential for the co-doped material as color-tunable phosphors for white-LEDs.

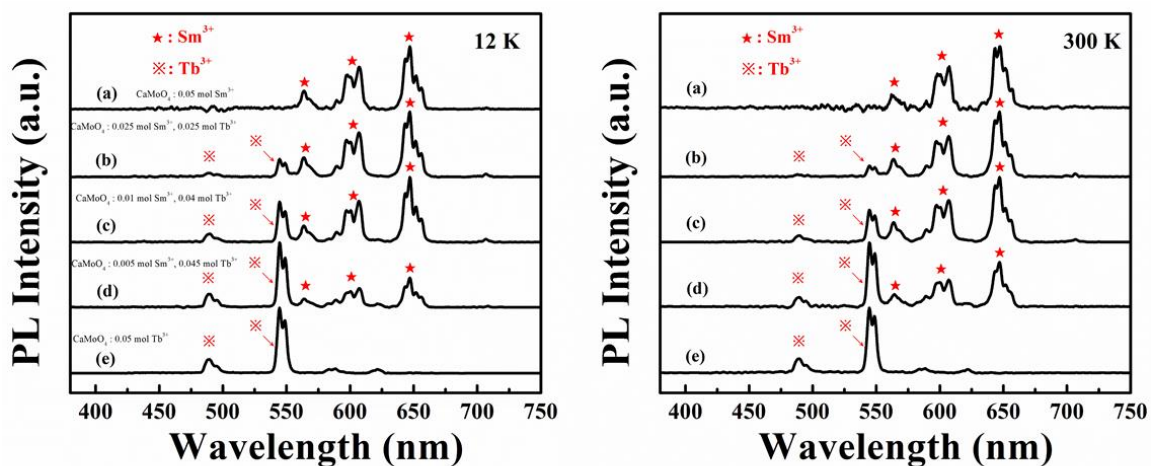


Figure 4. Spectra of 12 and 300 K PL with a molar ratio of (a) 0.05:0, (b) 0.025:0.025, (c) 0.01:0.04, (d) 0.005:0.045, and (e) 0:0.05.

Figure 5 shows the CIE coordinate of CaMoO_4 phosphors doped with different molar ratio of $\text{Sm}^{3+}/\text{Tb}^{3+}$ ions, which are calculated from its PL spectra at 12 and 300 K, respectively [24,25].

The calculated CIE chromaticity coordinates of the synthesized samples using the distribution of the PL emissions are presented as Figure 5. The CIE coordinates for sample a (0.05 mol Sm^{3+} -doped CaMoO_4) is (0.5963, 0.4057) at 12 K and is (0.5906, 0.4087) at 300 K which are agreed to the red phosphor. On the other hand, the calculated CIE coordinates of sample e (0.05 mol Tb^{3+} -doped Ca-MoO_4) is (0.2956, 0.6181) at 12 K and is (0.2957, 0.6162) at 300 K which are that of green phosphor. The variations in the CIE coordinates for emission colors of $\text{Sm}^{3+}/\text{Tb}^{3+}$ co-doped CaMoO_4 phosphors at 12 K are calculated to be: $\text{Sm}^{3+}/\text{Tb}^{3+} = 0.025/0.025$, $(x, y) = (0.5391, 0.4351)$; $\text{Sm}^{3+}/\text{Tb}^{3+} = 0.010/0.040$, $(x, y) = (0.5085, 0.4627)$; and $\text{Sm}^{3+}/\text{Tb}^{3+} = 0.005/0.045$, $(x, y) = (0.4205, 0.5289)$. For the 300 K measurements, CIE coordinates are $\text{Sm}^{3+}/\text{Tb}^{3+} = 0.025/0.025$, $(x, y) = (0.5518, 0.4279)$; $\text{Sm}^{3+}/\text{Tb}^{3+} = 0.010/0.040$, $(x, y) = (0.5166, 0.4560)$; and $\text{Sm}^{3+}/\text{Tb}^{3+} = 0.005/0.045$, $(x, y) = (0.4577, 0.5088)$. The adjustability of the chromaticity coordinates through the tuning of the molar ratio of $\text{Sm}^{3+}/\text{Tb}^{3+}$ ions under UV radiation, thus showing a great potential for their use in display and white-LEDs applications.

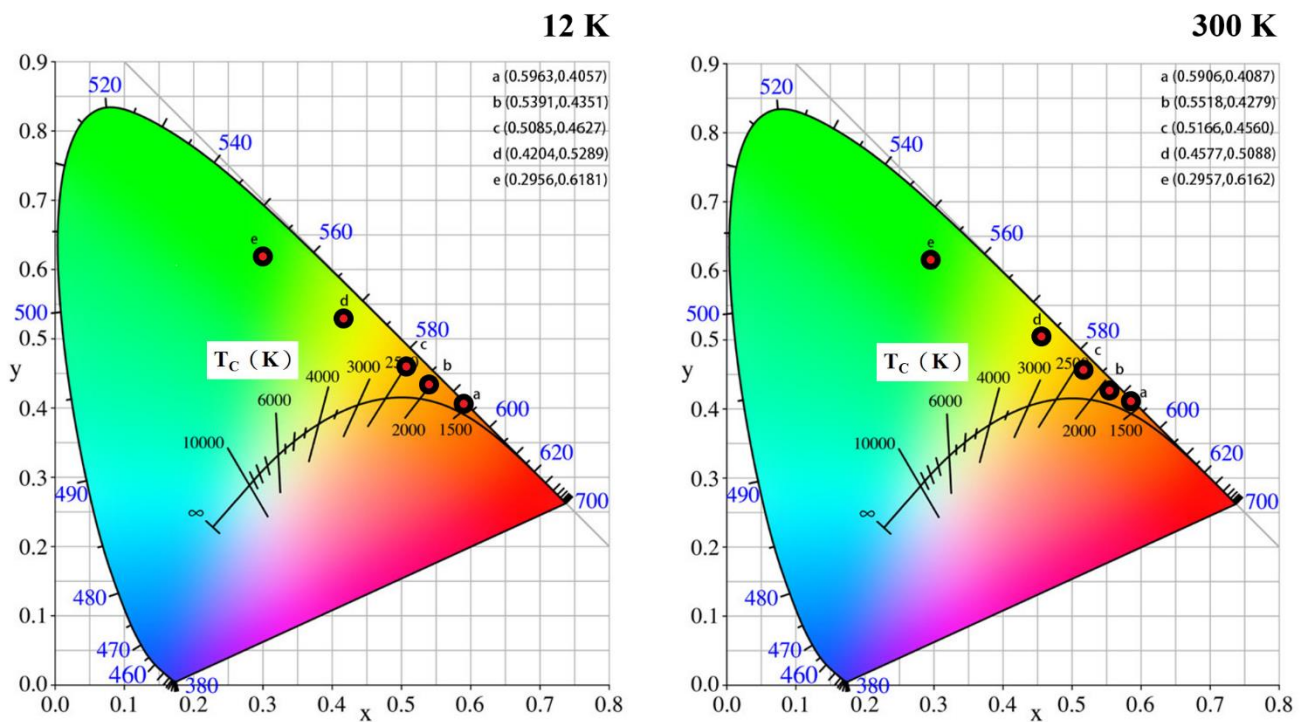


Figure 5. CIE coordinate of CaMoO_4 doped with different molar ratio of $\text{Sm}^{3+}/\text{Tb}^{3+}$ ions calculated based on their 12 and 300 K PL spectra.

4. Conclusions

In summary, we successfully synthesized a series of $\text{Sm}^{3+}/\text{Tb}^{3+}$ co-doped CaMoO_4 phosphors using an efficient microwave-assisted heating method. The XRD patterns evidence the crystallinity of the synthesized CaMoO_4 phosphors exhibiting a good tetragonal phase. The PL spectra of the synthesized $\text{Sm}^{3+}/\text{Tb}^{3+}$ co-doped CaMoO_4 show merits of multicolor emissions in the visible region, and the intensity ratio of the red/green emission obviously depends on the molar ratio of $\text{Sm}^{3+}/\text{Tb}^{3+}$ -co-doping. The variations in CIE coordinates of $\text{Sm}^{3+}/\text{Tb}^{3+}$ co-doped CaMoO_4 phosphors display the potential capability of the tunable emission for application in white-LEDs.

Author Contributions: Investigation, Y.-W.L. and W.H.; Supervision, K.-K.T.; Writing—original draft, W.-T.W.; Writing—review & editing, S.-Y.H. and Y.-C.L. All authors have read and agreed to the published version of the manuscript.

Funding: This research was funded by the Ministry of Science and Technology, Project No. MOST 108-2637-E-236-001 and 109-2637-E-236-001.

Conflicts of Interest: The authors declare no conflict of interest.

References

1. Yu, H.; Li, Z.; Lee, A.J.; Li, J.; Zhang, H.; Wang, J.; Pask, H.; Piper, J.; Jiang, M. A continuous wave SrMoO_4 Raman laser. *Opt. Lett.* **2011**, *36*, 579–581. [CrossRef] [PubMed]
2. Jiang, H.; Rooh, G.; Kim, H.J.; Park, H.; So, J.H.; Kim, S.; Kim, Y.D.; Zhang, W. Growth and scintillation characterizations of SrMoO_4 single crystals. *J. Korean Phys. Soc.* **2013**, *63*, 2018–2023. [CrossRef]
3. Pandey, I.R.; Kim, H.; Kim, Y. Growth and characterization of $\text{Na}_2\text{Mo}_2\text{O}_7$ crystal scintillators for rare event searches. *J. Cryst. Growth* **2017**, *480*, 62–66. [CrossRef]
4. Ahmed, N.; Kraus, H.; Kim, H.J.; Mokina, V.; Tsiunra, V.; Wagner, A.; Zhydachevskyy, Y.; Mykhaylyk, V.B. Characterisation of tungstate and molybdate crystals ABO_4 ($A = \text{Ca, Sr, Zn, Cd}$; $B = \text{W, Mo}$) for luminescence lifetime cryothermometry. *Materialia* **2018**, *4*, 287–296. [CrossRef]
5. Kaur, P.; Kumar, R.; Davessar, S.; Khanna, A. Structural and optical characterization of Er-doped CaMoO_4 down-converting phosphors. *Acta Crystallogr. Sect. B Struct. Sci. Cryst. Eng. Mater.* **2020**, *B76*, 926–938. [CrossRef]

6. Singh, M.; Haq, W.U.; Bishnoi, S.; Singh, B.P.; Arya, S.; Khosla, A.; Gupta, V. Investigating photoluminescence properties of Eu³⁺-doped CaWO₄ nanoparticles via Bi³⁺ amalgamation for w-LEDs application. *Mater. Technol.* **2021**, *39*, 1051–1061.
7. Cao, C.; Yang, X.; Chen, X.; Xie, A. Enhanced emission of Eu³⁺ in lutetium tungsten molybdenum oxide phosphors: Synthesis, optical properties, thermal behavior, and LED packaging. *J. Lumin.* **2020**, *223*, 117269. [[CrossRef](#)]
8. Cavalli, E.; Boutinaud, P.; Mahiou, R.; Bettinelli, M.; Dorenbos, P. Luminescence Dynamics in Tb³⁺-Doped CaWO₄ and CaMoO₄ Crystals. *Inorg. Chem.* **2010**, *49*, 4916–4921. [[CrossRef](#)]
9. Zhai, Y.; Han, Y.; Zhao, X.; Yang, S.; Liu, H.; Song, P.; Jia, G. Microwave synthesis of CaMoO₄:Sm³⁺ orange reddish-emitting phosphors and its photoluminescence property. *J. Mater. Sci. Mater. Electron.* **2017**, *28*, 15208–15216. [[CrossRef](#)]
10. Thongtem, T.; Kungwankunakorn, S.; Kuntalue, B.; Phuruangrat, A.; Thongtem, S. Luminescence and absorbance of highly crystalline CaMoO₄, SrMoO₄, CaWO₄ and SrWO₄ nanoparticles synthesized by co-precipitation method at room temperature. *J. Alloy. Compd.* **2010**, *506*, 475–481. [[CrossRef](#)]
11. Karki, S.; Aryal, P.; Ha, D.; Kim, H.J.; Park, H.K.; Pandey, I.R. Synthesis, Luminescence and Optical Properties of a CaMoO₄ Nano-Powder Prepared by Using the Precipitation Method. *J. Korean Phys. Soc.* **2019**, *75*, 534–540. [[CrossRef](#)]
12. Liao, J.; Qiu, B.; Wen, H.; Chen, J.; You, W.; Liu, L. Synthesis process and luminescence properties of Tm³⁺ in AWO₄ (A = Ca, Sr, Ba) blue phosphors. *J. Alloys Compd.* **2009**, *487*, 758–762. [[CrossRef](#)]
13. Sczancoski, J.C.; Bomio, M.D.R.; Cavalcante, L.S.; Joya, M.R.; Pizani, P.S.; Varela, J.A.; Longo, E.; Li, M.S.; Andrés, J.A. Morphology and Blue Photoluminescence Emission of PbMoO₄ Processed in Conventional Hydrothermal. *J. Phys. Chem. C* **2009**, *113*, 5812–5822. [[CrossRef](#)]
14. Xu, C.; Zou, D.; Guo, H.; Jie, F.; Ying, T. Luminescence properties of hierarchical CaMoO₄ micro-spheres derived by ionic liquid-assisted process. *J. Lumin.* **2009**, *129*, 474–477. [[CrossRef](#)]
15. Wu, H.; Hu, Y.; Zhang, W.; Kang, F.; Li, N.; Ju, G. Sol-gel synthesis of Eu³⁺ incorporated CaMoO₄: The enhanced luminescence performance. *J. Sol-Gel Sci. Technol.* **2012**, *62*, 227–233. [[CrossRef](#)]
16. Xu, M.; Si, J.; Li, G.; Liu, Y.; Cai, G.; Zhang, J. Structure, tunable luminescence and thermal stability in Tb³⁺ and Eu³⁺ co-doped novel KBaIn₂(PO₄)₃ phosphors. *J. Lumin.* **2020**, *221*, 117115. [[CrossRef](#)]
17. Tranquilin, R.L.; Lovisa, L.X.; Almeida, C.R.R.; Paskocimas, C.A.; Li, M.S.; Oliveira, M.C.; Gracia, L.; Andres, J.; Longo, E.; Motta, F.V.; et al. Understanding the white-emitting CaMoO₄ co-doped Eu³⁺, Tb³⁺, and Tm³⁺ phosphor through experiment and computation. *J. Phys. Chem. C* **2019**, *123*, 18536–18550. [[CrossRef](#)]
18. Kuzmanoski, A.; Pankratov, V.; Feldmann, C. Microwave-assisted ionic-liquid-based synthesis of highly crystalline CaMoO₄:RE³⁺ (RE = Tb, Sm, Eu) and Y₂Mo₄O₁₅:Eu³⁺ nanoparticles. *Solid State Sci.* **2015**, *41*, 56–62. [[CrossRef](#)]
19. Shih, H.-R.; Chang, Y.-S. Structure and Photoluminescence Properties of Sm³⁺ Ion-Doped YInGe₂O₇ Phosphor. *Materials* **2017**, *10*, 779. [[CrossRef](#)]
20. Liu, Z.; Sun, X.; Xu, S.; Lian, J.; Li, X.; Xiu, Z.; Li, Q.; Di Huo, A.; Li, J.-G. Tb³⁺- and Eu³⁺-Doped Lanthanum Oxysulfide Nanocrystals. Gelatin-Templated Synthesis and Luminescence Properties. *J. Phys. Chem. C* **2008**, *112*, 2353–2358. [[CrossRef](#)]
21. Kaur, S.; Rao, A.; Jayasimhadri, M.; Jaiswal, V.V.; Haranath, D. Tb³⁺ ion induced colour tunability in calcium aluminosilicate phosphor for lighting and display devices. *J. Alloys Compd.* **2020**, *826*, 154212. [[CrossRef](#)]
22. Ansari, A.A.; Alam, M. Optical and structural studies of CaMoO₄:Sm, CaMoO₄:Sm@CaMoO₄ and CaMoO₄:Sm@CaMoO₄@SiO₂ core-shell nanoparticles. *J. Lumin.* **2015**, *157*, 257–263. [[CrossRef](#)]
23. Ren, Q.; Zhao, Y.; Wu, X.; Hai, O. The color tunable of Tb³⁺/Sm³⁺ co-doped phosphors through Tb³⁺ → Sm³⁺ energy transfer. *Polyhedron* **2020**, *192*, 114862. [[CrossRef](#)]
24. Dixit, P.; Chauhan, V.; Kumar, P.; Pandey, P.C. Enhanced photoluminescence in CaMoO₄:Eu³⁺ by Mn²⁺ co-doping. *J. Lumin.* **2020**, *223*, 117240. [[CrossRef](#)]
25. Song, S.; Si, J.; Zhang, J.; Cai, G. Structure, tunable luminescence and energy transfer in Tb³⁺ and Eu³⁺ co-doped Ba₃InB₉O₁₈ phosphors. *RSC Adv.* **2019**, *9*, 1029–1035. [[CrossRef](#)] [[PubMed](#)]